Nonuniversality of roughness exponent of quasistatic fracture surfaces

Mehdi Ansari-Rad,[1] S. Mehdi Vaez Allaei,[1,*] and Muhammad Sahimi[2,†]
[1]*Department of Physics, University of Tehran, Tehran 14395-547, Iran*
[2]*Mork Family Department of Chemical Engineering & Materials Science, University of Southern California, Los Angeles, California 90089-1211, USA*

(Received 9 May 2011; revised manuscript received 30 January 2012; published 15 February 2012)

Numerous experiments have indicated that the fracture front (in three dimensions) and crack lines (in two dimensions) in disordered solids and rocklike materials is rough. It has been argued that the roughness exponent ζ is universal. Using extensive simulations of a two-dimensional model, we provide strong evidence that if extended correlations and anisotropy—two features that are prevalent in many materials—are incorporated in the models that are used in the numerical simulation of crack propagation, then ζ will vary considerably with the extent of the correlations and anisotropy. The results are consistent with recent experiments that also indicate deviations of ζ from its supposedly universal value, as well as with the data from rock samples.

DOI: 10.1103/PhysRevE.85.021121 PACS number(s): 05.40.−a, 81.40.Np, 62.20.M−

I. INTRODUCTION

The fracture of materials is a problem of immense importance. It is of fundamental scientific interest due to its complexities, and its understanding and prevention have been issues of great interest, as fracture is encountered in a variety of practical situations and has important economic implications. Therefore, the nucleation and propagation of fracture in materials have been studied for a long time, both experimentally and theoretically, as well as by computer simulations [1,2].

In their original work, Mandelbrot *et al*. [3] argued that the fracture surface is rough and self-affine. An interesting and very intriguing feature of fracture surfaces, seen in experiments and computed by computer simulations, is the scaling of its roughness. The scaling is expressed by the power-law relation between the width $W(L)$ of the fracture surface and the size L of the window over which $W(L)$ is computed, where the width is defined by

$$W(L) = \left\langle \sum_j [h(r_j) - \langle h \rangle_L]^2 \right\rangle^{1/2}, \tag{1}$$

in which $h(r_j)$ is the height of the fracture surface at point r_j, and $\langle h \rangle_L$ is its average in a window of size L. For a rough self-affine fracture surface, one must have

$$W(L) \sim L^{\zeta}, \tag{2}$$

with ζ being the roughness exponent. In general, depending on the material and experiment, one may consider two roughness exponents. One is ζ_{3D}, which is the out-of-plane roughness exponent of a fracture front in a three-dimensional (3D) experiment, whereas the second one, ζ_{2D}, is the roughness exponent of 2D cracks. Mandelbrot *et al*. [3] provided evidence that the roughness exponent may be a measure of the mechanical strength of materials. Ever since their work, many groups have estimated the roughness exponent for a variety of materials.

Thus, experiments have been carried out with metals [4], glass [5], and ceramics [6]. Some experiments with large-scale 3D samples indicated a nearly universal exponent, $\zeta_{3D} \simeq 0.8$, for the out-of-plane roughness. On smaller length scales, a smaller exponent, $\zeta_{3D} \simeq 0.4$–0.6, was reported. It was conjectured [7] that $\zeta_{3D} \simeq 0.8$ is valid for large scales and at higher speeds of fracture propagation, whereas the lower estimates should be associated with smaller length scales, although measurements with silica glass [8] did not yield the small-scale value. Experiments with 2D samples, mostly papers, yielded [9] $\zeta_{2D} \simeq 0.6$–0.7.

Experiments with rock samples have also yielded conflicting results. The original experimental study [10] with granitic faults yielded $\zeta_{3D} \simeq 0.85$. It has been suggested that the roughness exponent may take on two distinct values, depending on the type of rock or rocklike samples. One is around 0.8 for such materials as glass, cement, granite, and tuff, and a second, around 0.5, is for sandstones [11], calcite [12] and sintered glass beads [8], although $\zeta_{3D} \simeq 0.75$–0.8 was also reported for sandstones [13]. Others [14,15], however, analyzed extensive data for a variety of rock joints and reported nonuniversal values of the roughness exponent in the range $0 < \zeta_{3D} \leqslant 0.85$. Computer simulations have also been carried out. An elastic model yielded [16] a roughness exponent of about 0.86. Another study [17] used the fuse model [18] (see below) and claimed the existence of *two* universal roughness exponents. One, ∼0.71, is supposedly for local roughness, and a second one, ∼0.87, is for the global scale. A different elastic model yielded [19] a roughness exponent of about 0.73.

The problem has also been studied theoretically. Hansen and Schmittbuhl [20] (see also Schmittbuhl *et al*. [21] and Alava and Zapperi [21]) suggested a stress-weighted percolation model in which a quadratic damage gradient is self-generated, which is somewhat similar to the scalar percolation model in a gradient [22]. They related the roughness exponent ζ to ν, which is the exponent that characterizes that power-law divergence of the percolation correlation length ξ_p near the percolation threshold p_c, i.e., $\xi_p \sim (p - p_c)^{-\nu}$, where p is the fraction of the unbroken (or conducting) bonds. The roughness exponent of an in-plane fracture front, slowly propagating along a heterogeneous interface embedded in

*smvaez@ut.ac.ir
†moe@iran.usc.edu

an elastic body, was predicted [21] to be $\zeta_{2D} = \nu/(1+\nu)$. Here, ν was estimated to be about 1.54, which is not the same as $\nu = 4/3$ for the standard 2D percolation. Hence, one obtains $\zeta_{2D} \sim 0.61$. Others [23] reported a variety of estimates, ranging from 0.395 to 0.48. Dynamic effects have also been studied [24], leading to a value of 0.5. Thus, despite a considerable body of work, there is no clear consensus on whether the roughness exponent is universal and, if it is, what its numerical value may be.

Most materials on which the experiments have been carried out, ranging from rock samples to printing paper, are anisotropic. In rock, the anisotropy manifests itself in the form of stratification (layering). Long fibers in paper give rise to an anisotropic microstructure. In addition, most, if not all, materials contain extended correlations in the spatial distributions of their local properties, such as the porosity, conductivity, and elastic constants. With a single exception [25], however, none of the previous simulations of crack propagation took into account the effect of such important morphological features.

In this paper, we provide strong evidence, obtained through extensive computer simulations of 2D systems, that when anisotropy and extended correlations are included in models of fracture propagation in disordered materials, the resulting roughness exponent will be *nonuniversal*. The range of the roughness exponent that we compute covers most of its reported experimental estimates. As such, our results may go a long way toward settling the issue of the universality of the roughness exponent.

The rest of this paper is organized as follows. In the next section, we describe the details of the model and the numerical simulations that are used in this study. Section III describes the methods of estimating the roughness exponent. The results are presented and discussed in Sec. IV, and are compared with the experimental data in Sec. V. The paper is summarized in Sec. VI, where we also discuss future directions in this active area of research.

II. THE MODELS AND DETAILS OF NUMERICAL SIMULATIONS

A network of Hookean springs with natural length of zero can be mapped onto a resistor network [26]. Thus, we use the fuse model [18], which is a network of resistors that can burn out and turn into insulators representing microfractures, as a simple model of fracture in elastic media. One may, of course, question whether the results obtained with a scalar model are applicable to fracture in real materials, which represent a tensorial problem. While the precise values of the roughness exponents for the scalar and tensorial models might not be the same, past experience [1], 2] indicates that the qualitative features of the two classes of models are completely similar.

It is known that lattice anisotropy may affect the estimates of the roughness exponent [27] and, in fact, Ref. [25] used a square lattice that is anisotropic when studying vector and tensorial phenomena, such as fracture propagation. Therefore, triangular networks of resistors were used in order to ensure that no artificial lattice anisotropy affects the results. To ensure that the results do not depend on the method by which the microfractures are generated, two methods of burning out the resistors were used in the simulations.

In one model, the resistors were Ohmic, each characterized by a conductance g selected from a statistical distribution. There is strong experimental evidence that the fractional Brownian motion (FBM) provides an accurate description of the spatial distribution of the porosity, hydraulic conductance [28], and elastic moduli [29] of many porous materials, both at laboratory [30] and much larger scales [28,29]. Therefore, we selected the conductance of the resistors from the FBM, which is a self-affine fractal distribution that generates extended correlations. The most convenient representation of a FBM is by its power spectrum, which in 2D is given by

$$S(\boldsymbol{\omega}) = \frac{a}{\left(\omega_x^2 + \omega_y^2\right)^{H+1}}, \tag{3}$$

where a is a constant, and $\boldsymbol{\omega} = (\omega_x, \omega_y)$, with ω_i being the Fourier component in the ith direction. Here, H is the Hurst exponent such that $H > 1/2$ ($< 1/2$) implies positive (negative) correlations among the successive increments of the values generated by a FBM, while $H = 1/2$ represents the usual Brownian (random) case. To generate anisotropy and to introduce a cutoff length scale for the extent of the correlations, we rewrite $S(\boldsymbol{\omega})$ as

$$S(\boldsymbol{\omega}) = \frac{a}{\left(\omega_c^2 + \eta_x \omega_x^2 + \eta_y \omega_y^2\right)^{H+1}}, \tag{4}$$

where η_x and η_y are constant, which we refer to as the anisotropy parameters. Setting $\eta_y = 1$ and varying $\eta_x < 1$ generates layers (anisotropy) that are essentially parallel to the x direction, and vice versa. The larger the anisotropy parameters, the higher the number of the layers and, hence, the more anisotropic are the media. Here, ω_c is a cutoff frequency that defines a cutoff length scale ξ for the correlations: for all length scales ℓ such that for $\ell < \xi = 1/\omega_c$, the resistors' conductances are correlated, whereas for $\ell > \xi$, the correlations are lost. References [2,28–30] describe the methods by which the correlation length in materials and rock may be estimated.

A voltage difference was then applied to the network in one direction, a periodic boundary condition was used in the second direction, and the nodal voltage distribution in the network was determined using a variation of the conjugate-gradient method [31]. At each stage of the simulations, the resistor with the largest voltage drop was burnt out irreversibly. The voltage distribution was then recomputed, the next fuse was burnt out, and so on.

In the second model of simulating fracture propagation, a resistor burns out if the voltage difference across it exceeds a predefined threshold. In this case, it was the thresholds that were distributed according to the anisotropic FBM with a cutoff length scale for the correlations. Our simulations indicated that the roughness exponents for the two cases are identical. We used networks of size 300×300, and averaged the results over up to 120 realizations of the network.

III. CALCULATION OF THE ROUGHNESS EXPONENT

We focus on computing ζ_{2D}, but for the sake of brevity, we use ζ to denote the computed roughness exponent. To ensure

the accuracy of the results, we used two methods to estimate ζ. In one, we computed the width of the crack line defined by Eq. (1) and estimated ζ using Eq. (2). In the second method, we used the front-front correlation function defined by

$$C(r) = \langle [h(r_j) - h(r_j + r)]^2 \rangle, \tag{5}$$

where the averaging for each value of r is over all values of r_j. For a self-affine rough crack line, one must have

$$C(r) \sim r^{2\zeta}. \tag{6}$$

All of the estimates of ζ obtained by the two methods turned out to be consistent with each other, hence confirming their accuracy. We also used a third method to estimate the roughness exponent for a few cases, which will be described later in this paper.

IV. RESULTS AND DISCUSSIONS

Figure 1 presents the cracks lines for the case in which the direction of the line (from left to right) is aligned with the layers. The results are for two values of the correlation length, $\xi = 9$ and 15 (measured in units of the lattice bonds' length), and for $H = 0.5$. Because the crack line is more or less aligned with the layers, it is not very tortuous. Figure 2 presents the crack line for the same correlation lengths ξ as in Fig. 1, but for the case in which the direction of the crack line (from left to right) is perpendicular to the layers. In this case, the contrast between the layers gives rise to a very tortuous crack line. Increasing the correlation length also increases the length of the crack line that spans from one side of the lattice to the opposite side. Figures 1 and 2 already indicate the strong effect of anisotropy and extended correlations on the shape of the crack line.

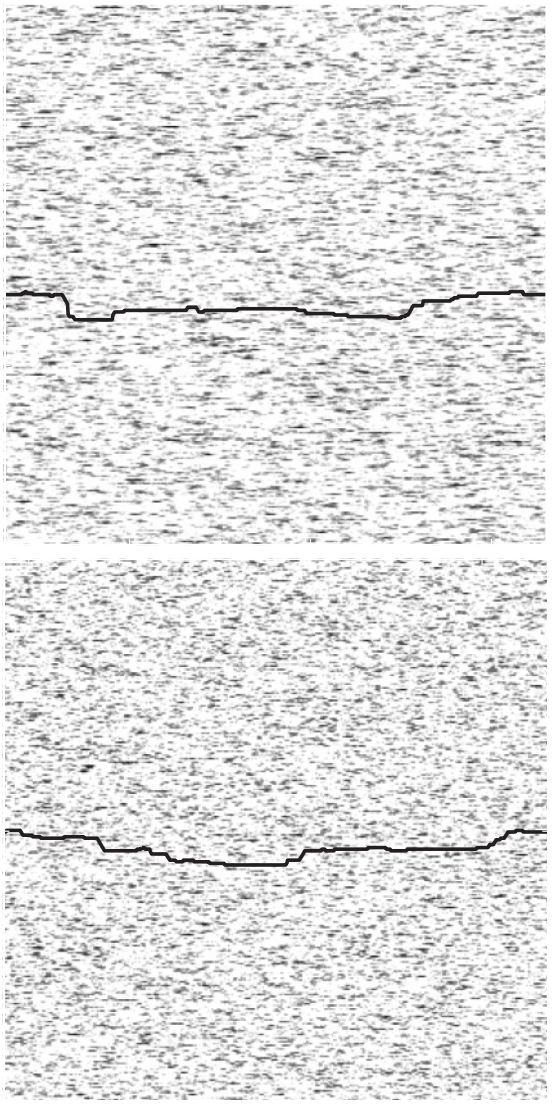

FIG. 1. Fracture front in the medium in which the overall direction of the front (from left to right) is parallel to the layers. The patterns are for the correlation lengths $\xi = 9$ (top) and 15 (bottom), and the anisotropy parameters $\eta_x = 0.01$ and $\eta_y = 1$.

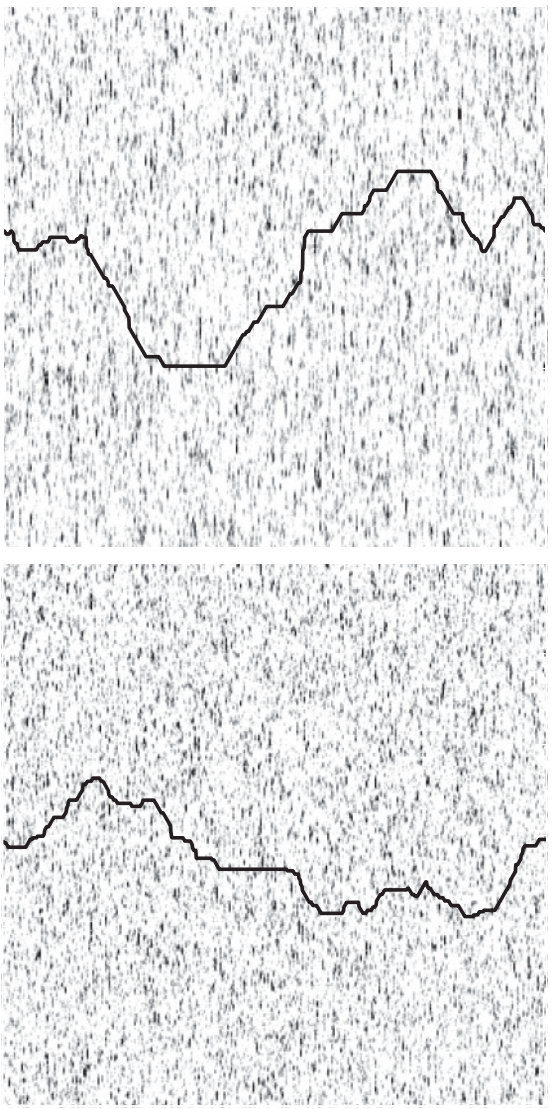

FIG. 2. Fracture front in the medium in which the overall direction of the front is perpendicular to the layers. The patterns are for correlation lengths $\xi = 9$ (top) and 15 (bottom), and the anisotropy parameters $\eta_x = 1.0$ and $\eta_y = 0.01$.

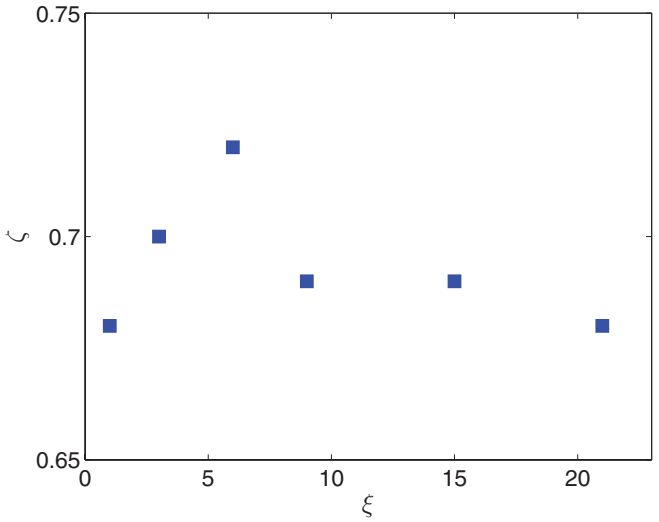

FIG. 3. (Color online) The dependence of the roughness exponent ζ on the extent of the correlations ξ. The medium is isotropic.

It has been claimed that the roughness exponent of the fracture front in 3D is universal. Although the experimental measurement of ζ_{2D} is more difficult, it has been claimed, based on computer simulations [17,27], that $\zeta_{2D} = \zeta$ is also universal. This claim is now checked against the results of our computer simulations. To estimate ζ, we first studied the isotropic case, but with a variety of correlation length ξ. Figure 3 presents the results. The roughness exponent does depend on the correlation length, hence providing a clue to its possible nonuniversality. Table I compiles all of the results for ζ, computed by the two methods described earlier, together with their estimated errors. The estimates of the roughness exponents, computed by the two methods, are close to one another. Bakke and Hansen [32] studied various methods of estimating the roughness exponent, and showed that they do not necessarily yield the same estimates, although they are usually very close to one another.

TABLE I. Roughness exponent ζ for fracture in isotropic media, computed for various correlation lengths using the window method (WM), namely, scaling of the width of the fracture front with window size, and the correlation function (CF) methods.

ξ	WM	CF
1	0.686 ± 0.003	0.679 ± 0.003
3	0.692 ± 0.003	0.706 ± 0.004
6	0.736 ± 0.004	0.713 ± 0.005
9	0.71 ± 0.005	0.69 ± 0.007
15	0.72 ± 0.006	0.69 ± 0.005
21	0.72 ± 0.006	0.68 ± 0.006

We then studied crack lines in anisotropic media with a cutoff correlation length. In effect, the extended but finite correlations divide the medium into two parts: the correlated part with an extent ξ around every bond of the lattice, and the random part outside of this region. In the correlated region with $H > 0.5$, the breaking thresholds, or the conductances, are positively correlated, and the tip of the growing crack sees its local neighborhood as more or less homogeneous. As the extent of the correlations increases, it becomes increasingly difficult for the crack tip to "see" the bonds outside of the correlated domain. It is then the anisotropy that plays the more important role. But, when $H < 0.5$, both the negative correlations and the anisotropy play equally important roles in the precise estimate of ζ.

Figure 4 presents the results for the width $W(L)$ of the crack line versus the length of the window L over which $W(L)$ was

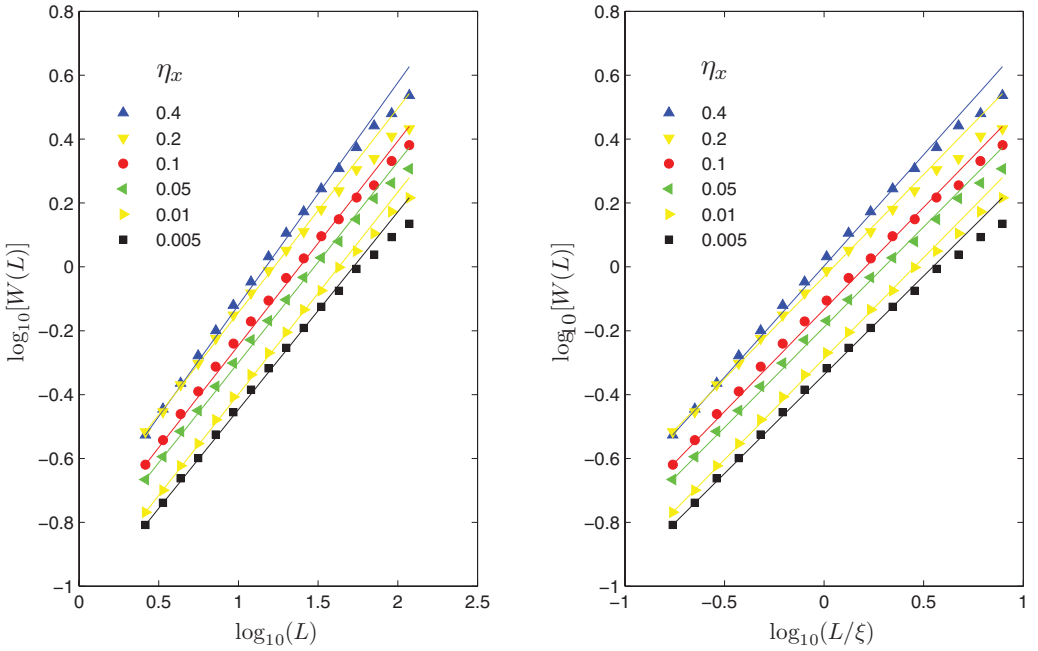

FIG. 4. (Color online) Left panel: Scaling of the width $W(L)$ of the fracture front with the window size L. Right panel: The same as the left panel, except that the window size L has been rescaled with the correlation length ξ. The lines represent the best fit of the data.

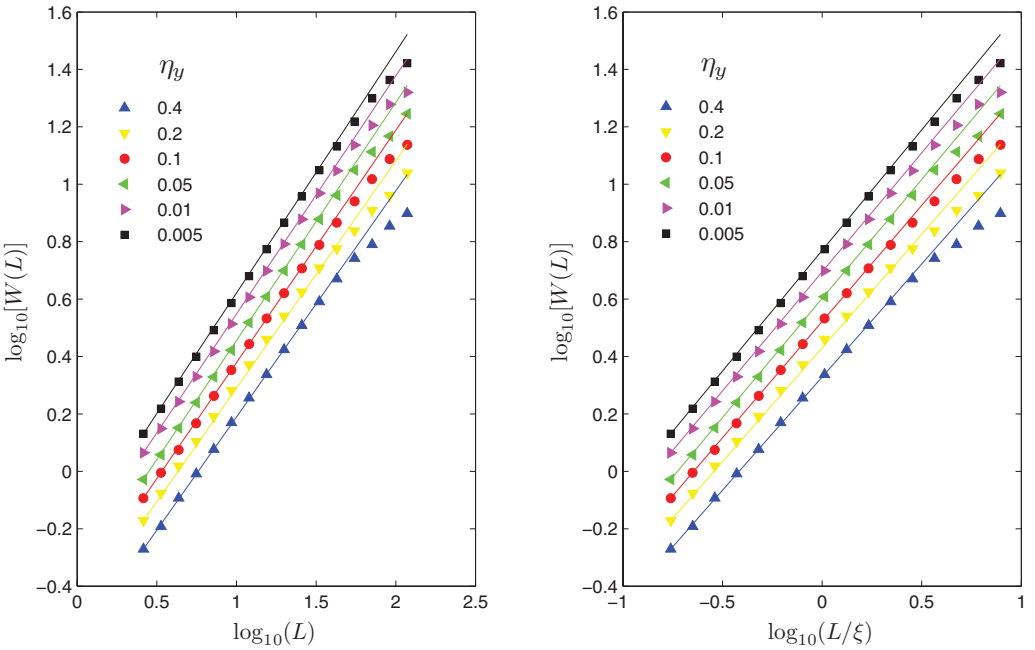

FIG. 5. (Color online) Same as in Fig. 4, but for the case in which $\eta_x = 1$ and η_y is varied.

computed, for the case in which $\eta_y = 1$ and η_x was varied. The correlation length is $\xi = 9$. The power law (4) is followed over nearly two orders of magnitude variations in L. If we rescale L with the correlation length ξ, then the same type of scaling is obtained, which is also shown in Fig. 4. Hence, the correlation length is relevant and its effect does not cancel if L is normalized with respect to it.

Figure 5 presents the results for the case in which $\eta_x = 1$ and η_y was varied, with the correlation length ξ being 9 again. Once again, the power law (4) is followed by the results over nearly two orders of magnitude variations in L. The normalization of L with respect to ξ neither changes the scaling of $W(L)$ with L, nor restores the presumed universality of roughness exponent ζ.

Figure 6 presents the computed roughness exponents for a range of the correlation length and the anisotropy parameters. For the case in which $\eta_y = 1$ and the direction of the crack line is more or less aligned with the layers, as shown in Fig. 4, decreasing η_x toward 0 decreases the roughness exponent from a high of about 0.7 toward 0.55. On the other hand, when $\eta_x = 1$ and the crack line is perpendicular to the layers, as shown in Fig. 5, ζ begins with a value close to 0.85 and decreases toward 0.7 with increasing η_y. Thus, taken together, one has $0.55 \leqslant \zeta \leqslant 0.85$, implying that ζ is nonuniversal. Table II compares the estimates of the roughness exponents ζ, computed by the two aforementioned methods.

If one defines the height difference Δh by

$$\Delta h(L) \equiv h(r_j + L) - h(r_j) - \langle h(r_j + L) - h(r_j) \rangle_j, \quad (7)$$

for a window of size L, then Bouchbinder *et al.* [33] (see also Santucci *et al.* [34]) suggested that one should study the probability density function (PDF) $P(\Delta h)$ by plotting $\ln[P(\Delta h)\sigma]$ versus $\Delta h/\sigma$, where σ is the standard deviation of the distribution. If the fracture front (in 3D) or the crack line (in 2D) is self-affine, then the PDF will be Gaussian and, therefore, the semilogarithmic plot of the PDF will be a parabola. However, if the fronts or crack line are multiaffine, then the tail of the PDF should deviate from a parabola. Such deviations have been reported in the experimental data for paper [33–35] and sandblasted Plexiglas (PMMA) [34], as well as in models of fracture in isotropic materials [17]. In addition, one may construct a structure function $S_n(L)$, defined by

$$S_n(L) \equiv \langle |h(r_j + L) - h(r_j)|^n \rangle_j, \quad (8)$$

which follows the scaling law

$$S_n(\lambda L) \sim \lambda^{\zeta_n} S_n(L), \quad (9)$$

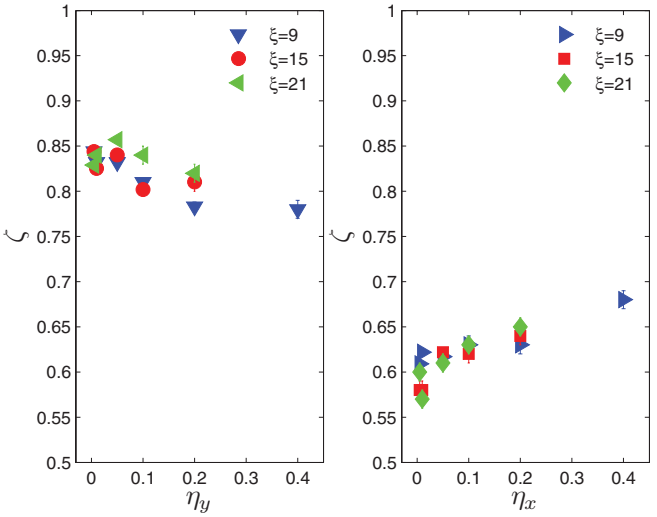

FIG. 6. (Color online) The estimated roughness exponent ζ and its dependence on the anisotropy parameters and extent of the correlations, ξ.

TABLE II. Roughness exponent ζ computed for the cutoff length $\xi = 9$ using the scaling of the width of the fracture surface (WM) and the correlation function (CF) methods.

	WM		CF	
η (x or y)	x	y	x	y
0.4	0.697 ± 0.005	0.788 ± 0.005	0.669 ± 0.005	0.764 ± 0.005
0.2	0.64 ± 0.005	0.792 ± 0.004	0.61 ± 0.006	0.780 ± 0.005
0.1	0.64 ± 0.007	0.809 ± 0.003	0.610 ± 0.005	0.810 ± 0.003
0.05	0.628 ± 0.005	0.829 ± 0.002	0.605 ± 0.004	0.834 ± 0.003
0.01	0.633 ± 0.005	0.829 ± 0.002	0.612 ± 0.003	0.835 ± 0.002
0.005	0.619 ± 0.004	0.840 ± 0.002	0.598 ± 0.004	0.847 ± 0.002

such that $\zeta_2/2 = \zeta$, with ζ being the roughness exponent that we have computed. For a multiaffine structure, $\zeta_n \neq n\zeta_2/2$, so that for each n the structure function is characterized by a distinct exponent $\zeta_n(n)$.

Thus, we constructed the PDFs for four cases, namely, the random and isotropic, correlated and isotropic, and the two correlated and anisotropic cases studied earlier, each for three window sizes, i.e., $L = 32$, 64, and 96. The results are presented in Fig. 7. The parabolas shown are the result of fitting the data for $L = 64$. As Fig. 7 indicates, the largest deviations from the parabola are obtained for the correlated systems, for both the isotropic and anisotropic cases. Note that to obtain a single-valued function, one must remove the dangling bonds at the end of the simulations, but doing so generates jumps in the crack line profile and destroys [17] its multiaffinity, giving rise to a Gaussian PDF.

Clearly, the structure function S_n can be computed for a variety of n, from which the exponent $\zeta_n(n)$ can be estimated. The results for this are shown in Fig. 8. They may be fitted to the quadratic form $\zeta_n(n) = n\zeta - n^2\lambda$, which are also shown in Fig. 8, along with a linear plot for small n. Note that since there is no reason to believe that ζ_n should depend on n quadratically, the estimated errors represent only those for the fitting to this particular quadratic form. The results

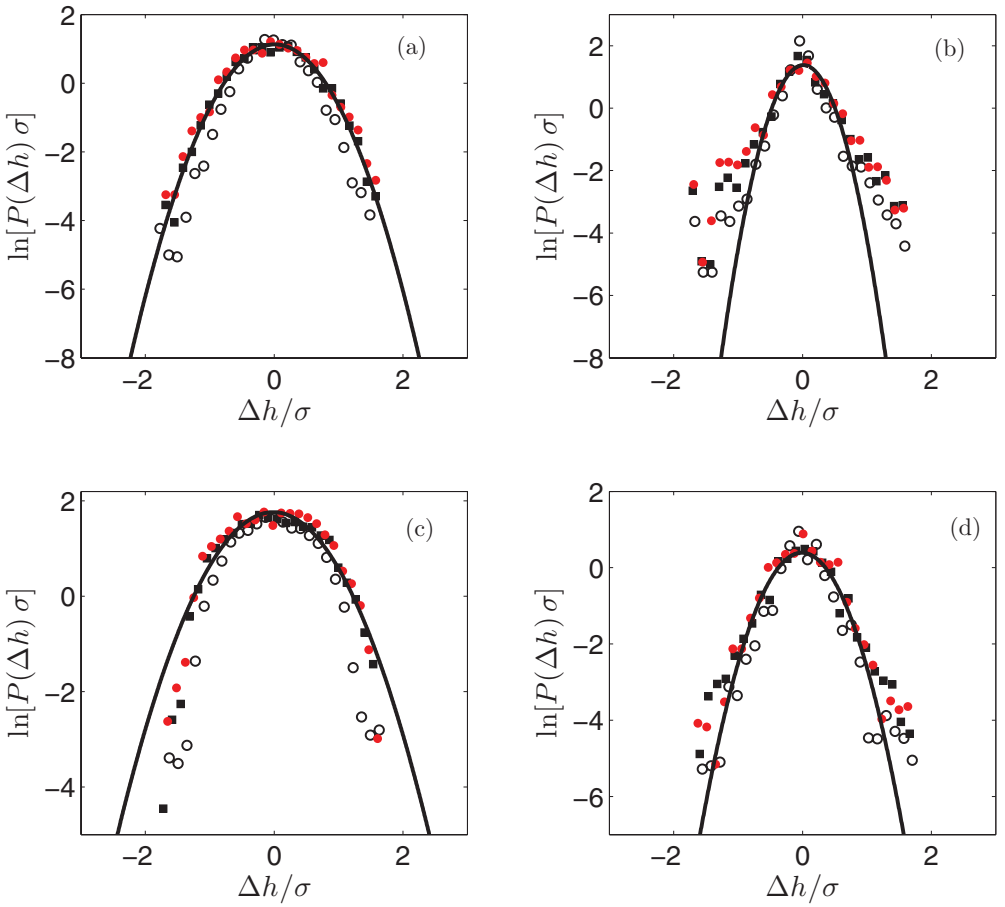

FIG. 7. (Color online) The probability distribution function $P(\Delta h)$ vs $\Delta h/\sigma$. (a) Uncorrelated and isotropic. (b) Correlated and isotropic with a correlation length $\xi = 9$. (c), (d) Anisotropic and correlated.

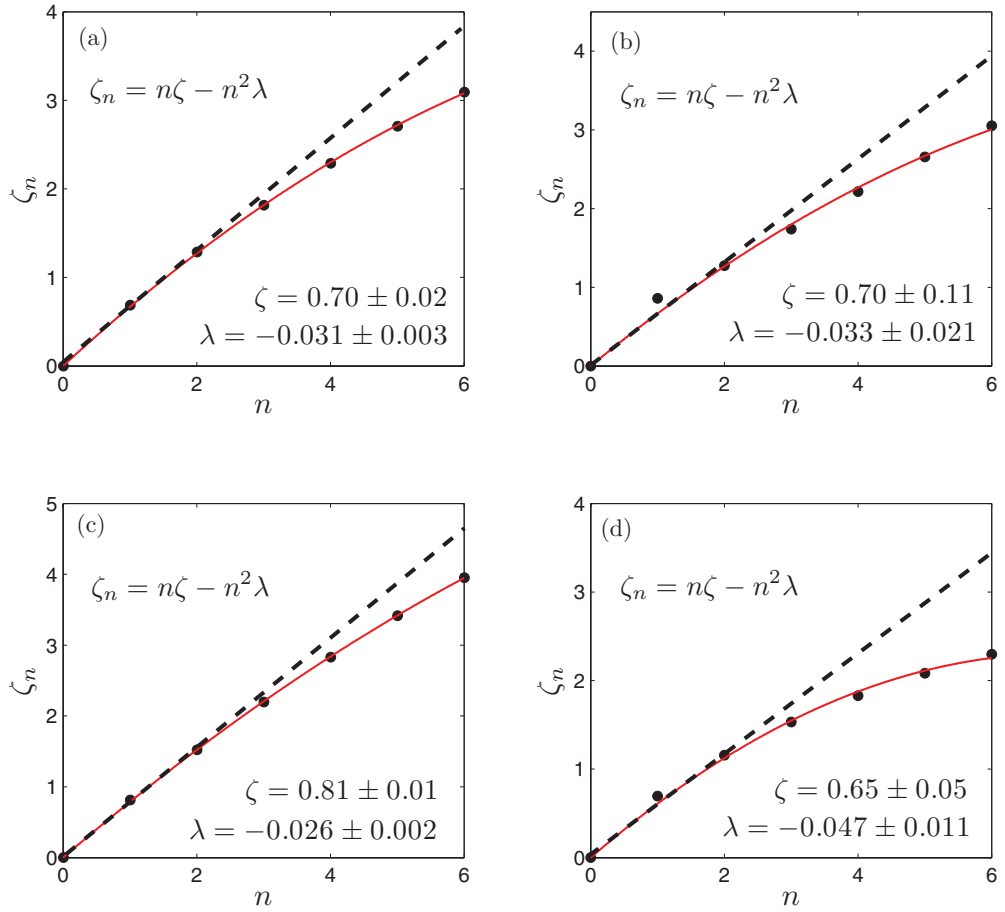

FIG. 8. (Color online) The dependence of the exponent ζ_n, characterizing the structure function S_n, on n. The four cases are the same as in Fig. 7.

for the two anisotropic cases were computed for $L = 9$, and $\eta_x = 0.01$ ($\eta_y = 1$), and for $\eta_y = 0.01$ ($\eta_x = 0.01$). As indicated in the figure, the two anisotropic cases yield values of ζ that are consistent with those presented in Table II.

Is it surprising that anisotropy and correlations affect the scaling? According to the current understanding of fracture [12,36], particularly in 3D, it is the failure mechanism, not a material's microstructure, that dictates the value of the roughness exponent, leading to universal ζ: in quasibrittle fracture that occurs on length scales on the order of the size of the fracture process zone (FPZ), $\ell_{\rm FPZ}$, the roughness exponent is about 0.8, whereas in brittle fracture that occurs on length scales larger than $\ell_{\rm FPZ}$, one has $\zeta \simeq 0.5$. Our simulations, on the other hand, indicate that, at least in 2D, it is the material's microstructure that dictates the value of the roughness exponent, and the growth of the crack line occurs at the tip due to stress concentration, implying that the FPZ is small and, thus, the failure mechanism is the same in all cases studied, regardless of the direction of the anisotropy relative to the crack line. Therefore, at least in this respect, our results are surprising and against the current understanding, and give rise to new questions that deserve to be studied.

One may ask why there is no change in the behavior on length scales below and above the correlation length ξ. As mentioned earlier, according to the current theories [12,36], the roughness exponent for fracture in a 3D material should be different on length scales smaller and larger than $\ell_{\rm FPZ}$. In the present study, the model material is 2D, and it is not clear why such a transition from one type of behavior to another should necessarily exist. Indeed, using 2D models, Nukala *et al.* [17] studied systematically the effect of the FPZ on the roughness exponent, but reported ζ to be independent of $\zeta_{\rm FPZ}$, with no transition from one type of behavior to another. Moreover, there is no direct link between the correlation length ξ and the size of the FPZ. In fact, even if ξ is not too large, one always has $\xi \gg \ell_{\rm FPZ}$ and, thus, the system is almost always on one side of the transition line.

We note that the roughness exponent ζ is the same as the Hurst exponent H that characterizes the nature of long-range correlations in the crack line, such that $H > 1/2$ ($H < 1/2$) implies positive (negative) correlations, whereas $H = 1/2$ corresponds to the random case with no correlations. As long as the material is isotropic with a random (uncorrelated) microstructure, the roughness exponent $\zeta > 1/2$, which implies long-range positive correlations. For uncorrelated and

isotropic systems, Bouchbinder *et al*. [37] suggested a mechanism that explains why $H > 1/2$. In their model, quasistatic fracture happens by void formation and coalescence. There is a length scale R that determines where voids nucleate. The entire fracture process then consists of rapid growth steps, interrupted by the slower void nucleation. As long as $R \neq 0$, one has positive correlations. If, however, the growth takes place right at the crack tip [24] ($R = 0$), then the positive correlations are lost, and $H = \zeta = 1/2$.

The mechanism suggested by Bouchbinder *et al*. [37] should presumably be applicable to the case in which the system is correlated, but the correlation length ξ is not too large, hence allowing ℓ_{FPZ} to be non-negligible. But, when the correlation length ξ is very large, then, regardless of whether or not the material is isotropic, the proposed mechanism should no longer be valid because cracking is no longer quasibrittle. Moreover, when the crack line moves more or less in the direction of the layers, one must have positive correlations, but not when it does not move in that direction. Thus, our work has given rise to important new questions that deserve to be studied.

V. COMPARISON WITH EXPERIMENTAL DATA

There is experimental evidence that supports the nonuniversality of ζ. One piece of evidence is provided by rock samples [15], as already mentioned. Further evidence is provided by the work of Menezes-Sobrinho *et al*. [38], who studied the rupture of five types of paper. They subjected the samples to a uniaxial force and studied fracture of the papers along two orthogonal directions. According to Ref. [39], "The machine-made paper has a strong directional preference. This anisotropy is due to uneven fiber orientation and drying conditions." Indeed, in the experimental studies [40] of the characterization of paper by one of us (M.S.), such anisotropy was reported.

Menezes-Sobrinho *et al*. [37] reported that for at least three of the papers, the roughness exponent was dependent upon the direction with $0.58 \leqslant \zeta \leqslant 0.94$, and interpreted their results based on the alignment of the papers' fibers, i.e., the anisotropy. Earlier experiments with various papers [9] had yielded an average value, $\zeta \simeq 0.6$–0.7. These results are consistent with our estimates of ζ, if we view the layers in our model as an approximate representation of a paper's fibers.

VI. SUMMARY

The results presented in this paper provide strong evidence that contrary to the widely held belief, the roughness exponent is, in general, nonuniversal, at least in 2D, as was studied in this paper. We must also emphasize that without a finite but extended correlation in the distribution of the conductances or the breaking thresholds, one would not obtain the nonuniversality that we report here. In other words, *both* the correlations and the anisotropy contribute to the nonuniversality and are relevant.

The present study also indicates that contrary to the repeated assertions in the past that it is the failure mechanism that is responsible for the value of the roughness exponent, we find that at least in 2D, it is the microstructure of a material, and in particular its anisotropy and the existence of extended correlations, that control the value of the roughness exponent.

Finally, the results indicate that simulations similar to ours but in 3D disordered media must be carried out in order to estimate the roughness exponent. One may consider a variety of scenarios for the interplay between anisotropy and extended correlation in 3D materials. Thus, we suspect that in such a case, ζ may be nonuniversal even more strongly than in 2D media, including the possibility of being smaller than 0.5, and hence covering the entire range of ζ reported for some rock samples and other materials. But this remains to be seen; the simulation of a 3D system to study this possibility is currently in progress.

ACKNOWLEDGMENT

The work of S.M.V.A. was supported in part by the Research Council of the University of Tehran.

[1] M. J. Alava, P. K. V. V. Nukala, and S. Zapperi, Adv. Phys. **55**, 349 (2006).
[2] M. Sahimi, *Heterogeneous Materials II*, Chap. 5–8 (Springer, Berlin, 2003).
[3] B. B. Mandelbrot, D. E. Passoja, and A. J. Paullay, Nature (London) **308**, 721 (1984).
[4] K. J. Måløy, A. Hansen, E. L. Hinrichsen, and S. Roux, Phys. Rev. Lett. **68**, 213 (1992); E. Bouchaud, G. Lapasset, J. Planés, and S. Navéos, Phys. Rev. B **48**, 2917 (1993).
[5] P. Daguier, B. Nghiem, E. Bouchaud, and F. Creuzet, Phys. Rev. Lett. **78**, 1062 (1997).
[6] J. J. Mecholsky, D. E. Passoja, and K. S. Feinberg-Ringel, J. Am. Ceram. Soc. **72**, 60 (1989).
[7] For a review, see E. Bouchaud, Surf. Rev. Lett. **10**, 797 (2003).
[8] L. Ponson, D. Bonamy, and E. Bouchaud, Phys. Rev. Lett. **96**, 035506 (2006).
[9] J. Kertész, V. K. Horvath, and F. Weber, Fractals **1**, 67 (1993); T. Engoy, K. J. Måløy, A. Hansen, and S. Roux, Phys. Rev. Lett. **73**, 834 (1994); J. Rosti, L. I. Salminen, E. T. Seppälä, M. J. Alava, and K. J. Niskanen, Eur. Phys. J. B **19**, 259 (2001); L. I. Salminen, M. J. Alava, and K. J. Niskanen, *ibid*. **32**, 369 (2003).
[10] J. Schmittbuhl, S. Roux, and Y. Berthaud, Europhys. Lett. **28**, 585 (1994); J. Schmittbuhl, F. Schmitt, and C. Scholz, J. Geophys. Res. **100**, 5953 (1995).
[11] J. Schmittbuhl, S. Gentier, and S. Roux, Geophys. Res. Lett. **20**, 639 (1993).
[12] J. M. Boffa, C. Allain, and J. P. Hulin, Eur. Phys. J. **2**, 281 (1998); L. Ponson, H. Auradou, M. Pessel, V. Lazarus, and J. P. Hulin, Phys. Rev. E **76**, 036108 (2007).
[13] P. Gouze, C. Noiriel, C. Bruderer, D. Loggia, and R. Leprovost, Geophys. Res. Lett. **30**, 1267 (2003).
[14] M. Nasseri, B. Mohanty, and R. Young, Pure Appl. Geophys. **163**, 917 (2006).

[15] B. L. Cox and J. S. Y. Wang, Fractals **1**, 87 (1993); R. A. Johns, J. S. Steude, L. M. Castanier, and P. V. Roberts, J. Geophys. Res. **98**, 1889 (1993); N. E. Odling, Rock Mech. Rock Eng. **27**, 135 (1994).

[16] B. Skjetne, T. Helle, and A. Hansen, Phys. Rev. Lett. **87**, 125503 (2001).

[17] P. K. V. V. Nukala, S. Zapperi, M. J. Alava, and S. Simunović, Phys. Rev. E **76**, 056111 (2007); **78**, 046105 (2008).

[18] L. de Arcangelis, S. Redner, and H. J. Herrmann, J. Phys. Lett. (Paris) **46**, 585 (1985).

[19] I. Malakhovsky and M. A. J. Michels, Phys. Rev. B **74**, 014206 (2006); **76**, 144201 (2007).

[20] A. Hansen and J. Schmittbuhl, Phys. Rev. Lett. **90**, 045504 (2003).

[21] J. Schmittbuhl, A. Hansen, and G. G. Batrouni, Phys. Rev. Lett. **90**, 045505 (2003); M. J. Alava and S. Zapperi, *ibid.* **92**, 049601 (2004).

[22] B. Sapoval, M. Rosso, and J. F. Gouyet, J. Phys. Lett. (Paris) **46**, 149 (1985).

[23] D. Ertas and M. Kardar, Phys. Rev. E **49**, 2532 (1994); J. Schmittbuhl, S. Roux, J.-P. Vilotte, and K. J. Måløy, Phys. Rev. Lett. **74**, 1787 (1995); P. Chauve, P. Le Doussal, and K. J. Wiese, *ibid.* **86**, 1785 (2001); A. Rosso and W. Krauth, Phys. Rev. E **65**, 025101 (2002).

[24] S. Ramanathan, D. Ertas, and D. S. Fisher, Phys. Rev. Lett. **79**, 873 (1997); S. Ramanathan and D. S. Fisher, *ibid.* **79**, 877 (1997).

[25] X. Zhang, M. A. Knackstedt, D. Y. C. Chan, and L. Paterson, Europhys. Lett. **34**, 121 (1996).

[26] W. Tang and M. F. Thorpe, Phys. Rev. B **36**, 3798 (1987).

[27] Jan Øystein Haaving Bakke and A. Hansen, Phys. Rev. Lett. **100**, 045501 (2008).

[28] For a recent comprehensive review of the data for rock, see M. Sahimi, *Flow and Transport in Porous Media and Fractured Rock*, 2nd ed., Chap. 5 (Wiley-VCH, Weinheim, 2011); see also Ref. [2].

[29] M. Sahimi and S. E. Tajer, Phys. Rev. E **71**, 046301 (2005).

[30] M. A. Knackstedt, A. P. Sheppard, and W. V. Pinczewski, Phys. Rev. E **58**, R6923 (1998); M. A. Knackstedt, A. P. Sheppard, and M. Sahimi, Adv. Water Resour. **24**, 257 (2001).

[31] S. M. Vaez Allaei and M. Sahimi, Int. J. Mod. Phys. C **16**, 1 (2005).

[32] Jan Øystein Haaving Bakke and A. Hansen, Phys. Rev. E **76**, 031136 (2007).

[33] E. Bouchbinder, I. Procaccia, S. Santucci, and L. Vanel, Phys. Rev. Lett. **96**, 055509 (2006).

[34] S. Santucci, K. J. Måløy, A. Delaplace, J. Mathiesen, A. Hansen, Jan Øystein Haaving Bakke, J. Schmittbuhl, L. Vanel, and P. Ray, Phys. Rev. E **75**, 016104 (2007).

[35] S. Santucci, L. Vanel, and S. Ciliberto, Phys. Rev. Lett. **93**, 095505 (2004).

[36] D. Bonamy, L. Ponson, S. Prades, E. Bouchaud, and C. Guillot, Phys. Rev. Lett. **97**, 135505 (2007).

[37] E. Bouchbinder, J. Mathiesen, and I. Procaccia, Phys. Rev. Lett. **92**, 245505 (2004); see also, I. Afek, E. Bouchbinder, E. Katzav, J. Mathiesen, and I. Procaccia, Phys. Rev. E **71**, 066127 (2005).

[38] I. L. Menezes-Sobrinho, M. S. Couto, and I. R. B. Ribeiro, Phys. Rev. E **71**, 066121 (2005).

[39] L. Salminen, Ph.D. Thesis, Helsinki University of Technology, 2003.

[40] J. Ghassemzadeh and M. Sahimi, Chem. Eng. Sci. **59**, 2265 (2004); **59**, 2281 (2004).